ANALYTICAL SCIENCES FEBRUARY 2015, VOL. 31

Silicon Nanowire Biosensor for Highly Sensitive and Multiplexed Detection of Oral Squamous Cell Carcinoma Biomarkers in Saliva

Yulin ZHANG,* Rongmei CHEN, Lu XU,* Yong NING,* Shenggao XIE,*† and Guo-Jun ZHANG*†**

**School of Laboratory Medicine, Hubei University of Chinese Medicine, 1 Huangjia Lake West Road, Wuhan 430065, P. R. China*
***Qianjiang Central Hospital, 22 Zhanghua Road, Qianjiang 433100, Hubei Province, P. R. China*

Silicon nanowire (SiNW) field-effect transistor (FET) biosensors have already been used as powerful sensors for the direct detection of disease-related biomarkers. However, the multiplexed detection of biomarkers in real samples is still challenging. Interleukin 8 (IL-8) and tumor necrosis factor α (TNF-α) are two typical biomarkers of oral squamous cell carcinoma (OSCC). In this study, we developed a multiplexed detection methodology for IL-8 and TNF-α detection in saliva using SiNW FET biosensors. We fabricated the SiNW FET sensors using a top-down lithography fabrication technique. Subsequently, we achieved the multiplexed detection of two biomarkers in saliva by specific recognition of the two biomarkers with their corresponding antibodies, which were modified on the SiNW. The established method was found to have a limit of detection as low as 10 fg/mL in 1×PBS as well as 100 fg/mL in artificial saliva. Because of its advantages, including label-free and multiplexed detection, non-invasive analysis, highly sensitive and specific determination, the proposed method is expected to be widely used for the early diagnosis of OSCC.

Keywords Silicon nanowire, field effect transistor, biosensors, biomarker, detection, saliva

(Received October 30, 2014; Accepted December 19, 2014; Published February 10, 2015)

Introduction

Oral cancer is one of the six most common cancers worldwide. It is estimated that annually there are over 300000 oral cancer cases worldwide.[1] The oral squamous cell carcinoma (OSCC) accounts for over 90% of all oral cancers. According to the analysis of World Health Organization (WHO), OSCC has one of the leading mortality rates among all malignancies, with a 5-year mortality rate of approximately 50%.[2] Although 90% of OSCC is possible to be cured with early treatment, 70% of patients being diagnosed with oral cancers are at the last stage of cancer development.[2] Due to a lack of definite early symptoms and early diagnosis, the morbidity and mortality rates have remained high during the past 30 years.[3] It is meaningful and challenging to develop strategies to identify and detect OSCC at an early stage.

A biomarker of cancer refers to a molecular signature that provides either diagnostic or prognostic insight into disease progression.[4] Many researchers have achieved early diagnosis of cancer by studying biomarkers.[5] Several OSCC biomarkers in body fluids are found to be involved in the development of cancer in its early stage. Nevertheless, because no single biomarker could realize a high accuracy of identifying early disease onset, multiple biomarker candidates are used for the highly accurate detection of OSCC.[3,6] The levels of interleukin 8 (IL-8) and tumor necrosis factor α (TNF-α) found in the saliva of OSCC patients were shown to be significantly elevated compared to the control group,[7] which makes them potential biomarkers for the early diagnosis of OSCC. Similar to blood, saliva contains a vast variety of biomolecules with a potential for diagnostic applications. Saliva, as a diagnostic fluid, has many advantages over blood, such as its simple collection and processing, non-invasive nature, low cost and so on.[8] As of late, there have been a significant number of diseases shown to be diagnostically reflected in saliva.[9] However, the concentration of the biomarkers in saliva is much lower than that in the blood, and the salivary environment is more complicated, revealing that a sensitive and multiplexed detection method for biomarkers is highly required.[10]

These biosensors based on the labeling of biomolecules with tags, such as radioactive isotope, quantum dots or fluorescent dyes, have been applied for the detection of disease biomarkers.[11-14] Although these label-based methods have good sensitivity, they suffer from some drawbacks, including challenges concerning the labeling procedures, tedious and time-consuming experimental procedures, thereby hindering them from more extensive applications.[15] In an attempt to overcome the above disadvantages, several label-free sensor technologies have been employed to detect biomarkers, such as surface plasmon resonance (SPR),[16] a quartz crystal microbalance (QCM),[17] atomic force microscopy (AFM),[18] surface-enhanced raman spectroscopy (SERS),[19] and a field-effect transistor (FET).[20-25] Among them, the FET biosensors have recently attracted tremendous attention due to their remarkable advantages of high sensitivity.[26,27] The sensitivity of the biosensor is a critical parameter since the biomarkers in saliva are usually present at very low concentration.[28] Compared

† To whom correspondence should be addressed.
E-mail: zhanggj@hbtcm.edu.cn (G.-J. Z.); xiesg100@163.com (S. X.)

to other FET biosensors, the diameter of a silicon nanowire (SiNW) is comparable to the dimensions of many biological relevant molecules, offering an opportunity for efficient bioaffinity and high sensitivity in detecting biomarkers.[29] Again, thanks to the SiNW very small dimension, the SiNW obtains a high surface-to-volume ratio, allowing the SiNW FET biosensor to be a very sensitive tool for biomolecule detection.[30] At the same time, the biosensor could also realize multiplexed selective detection of biological species by means of functionalizing the SiNW FET with various biological receptors.[31] Lieber *et al.* reported the multiplexed detection of the disease-related protein biomarkers using the SiNW FET,[32] in which the multiplexed detection of prostate specific antigen (PSA), PSA-α1-antichymotrypsin, carcinoembryonic antigen and mucin-1 was realized in an undiluted serum sample by using SiNW arrays fabricated by the bottom-up approach.

Normally, The SiNW sensor chip can be fabricated by using of either bottom-up or top-down approaches.[32,33] The bottom-up fabrication is simple and cost-effective. However, it has difficulties concerning position and shape control.[34] On the contrary, the top-down approach can be compatible with the established complementary metal oxide semiconductor (CMOS) lithographic manufacturing technologies, capable of controlling the SiNW array in well-defined shape. In our study, the monocrystalline SiNW FET sensor chip was fabricated by a top-down approach, and used as a label-free biosensor for the multiplexed detection of OSCC biomarkers. By using a unique method to locate the antibody solution on the different SiNW array surfaces, the antibodies of TNF-α and IL-8 are selectively modified on the SiNW sensor array surfaces in our work. Because TNF-α and IL-8 have the opposite net charge at pH 8.5 of the buffer, the two biomarkers can be easily discriminated. Therefore, the highly sensitive, multiplexed and specific detection of TNF-α and IL-8 in the mimic saliva is successfully realized by the antibody-functionalized SiNW FET biosensor. The proposed SiNW FET biosensor used in this work has potential to be a diagnostic tool for the OSCC at a premature stage.

Experimental

Materials and reagents

Anti-human IL-8, recombinant human IL-8, mouse anti-human TNF-α, recombinant human TNF-α were purchased from Creative Biomart. All chemicals were purchased from Sigma-Aldrich with the exception of the amino-polyethylene glycol (amino-PEG, Fluka). Solutions were made with Milli-Q deionized water.

Silicon nanowire fabrication

The n-type SiNW biosensor was fabricated on an n-doped silicon-on-insulator (SOI) substrate using the top-down approach, as described in previously work.[35] The SOI wafers consist of 700 nm silicon and 145 nm buried oxide layers. The 5×10^{13} cm^{-2} doses of phosphorous dopants were implanted into the wafer at 30 keV and activated at 1000°C *via* rapid thermal annealing. A deep ultraviolet top-down lithography technique was performed to pattern and etch fins on a 50 – 80 nm silicon layer in order to produce nanowire arrays. The wafer underwent further thermal oxidation of the fin structure at 900°C in oxygen, O_2, for around 4 h to define the individual nanowires. Contact metal definition and Si_3N_4/SiO_2 passivation of metal lines were carried out. Lastly, SiNWs were released after dry etching of the Si_3N_4/SiO_2 passivation layers, followed by wet etching of the remaining SiO_2 on the surface. The SiNWs formed are in arrays of 90 µm long with 2 µm spacing in between 2 wires. The SiNWs arrays are divided into 4 sections, named A, B, C and D. All sections have 12 clusters containing 5 nanowires each, except for section D, which has 15 clusters. All nanowires present on the biosensing chip are individually addressable and fully compatible with CMOS technology. The design of the SiNW-based chip is shown in Fig. 1.

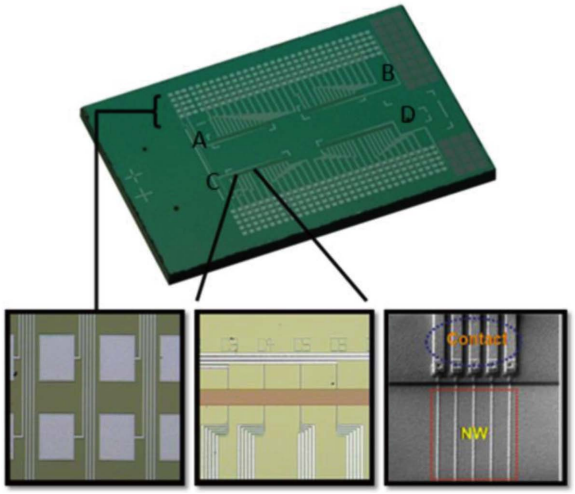

Fig. 1 Diagram showing the design of the SiNW-based FET biosensor chip. 4 different clusters are labeled with A, B, C and D, respectively. Magnified views of the contact pads, the contact lines and a cluster of SiNWs, respectively, are also shown.

Surface modification of SiNWs

The procedures of immobilizing the antibodies onto the nanowire array surfaces were conducted as described previously with a little modification.[21] After the surface was treated with 3-aminopropyltriethoxysilane (APTES) and glutaraldehyde, 100 µg/mL of antibodies (anti IL-8 and anti TNF-α) in a 1×phosphate buffer solution (PBS) were pipetted into each well and allowed to incubate in a moist environment for 2 h at room temperature. The unbounded antibodies were washed off with a buffer solution (1×PBS). The SiNW was then incubated overnight at 4°C with 0.01 mg/mL of amino-PEG in 1×PBS to passivate the unreacted aldehyde surface groups. The SiNW chip was later rinsed with water, dried with a stream of nitrogen gas, and immediately used for electrical measurements.

Artificial saliva preparation

The artificial saliva formula used in the present work is a modified version of the Fusayama protocol.[35] After 100 mL of ultrapure water was added in a 150 mL beaker, 0.4 g of mucin was added. The mixture was stirred until the mucin homogenously dissolved. This was followed by the addition of 0.4 g of urea, 0.06 g of sodium hydrogen phosphate (Na_2HPO_4), 0.06 g of anhydrous calcium chloride ($CaCl_2$), 0.04 g of potassium chloride (KCl) and 0.04 g of sodium chloride (NaCl) into the mixture. Using a pH meter, the pH of the solution was determined and corrected to 7.2 using an acidic/basic substance. The bottle containing the artificial saliva was sterilized by sending it for autoclaving. It was then stored in a fridge at 4°C until further use.

Electrical measurement

Electrical measurements were performed using an Alessi 9 REL-6100 probe station (Cascade Microtech, Beaverton, OR) coupled with an Agilent Technologies B1500A Semiconductor Device Analyzer, as described previously with a little modification.[35] The magnitude of current flowing through the drain (I_d) and the substrate (I_s) were measured and displayed as a current-voltage (I-V) graph on screen when the source electrode voltage had a range of –0.5 to 0.5 V with a step size of 0.05 V were swept. The values for resistance were obtained from the gradient of an I-V graph at 100 mV. Before any electrical measurement, a measuring buffer solution, 0.01×PBS at pH 8.5, was added to the SiNW device. After the first measurement of the resistance, which was performed before target binding (R1), the SiNW chips were rinsed with ultrapure water to remove any measuring buffer. The SiNW chips were dried using gaseous nitrogen. Targets were applied on SiNWs and incubated for a period of 1 h in a moist petri dish at room temperature, after which the SiNW chips were subjected to washing with 1×PBS and rinsing with ultrapure water. A fresh measuring buffer was applied onto the clean and dried SiNW chips. A second measurement of the resistance (R2) was then carried out. For each group, a total of 10 wires from 2 clusters were measured. The percentage change in resistance was then computed by using: $[(R2 - R1)/R1] \times 100\%$.

Results and Discussion

Sensing principles

In order to realize the multiplexed detection of the OSCC biomarkers, the SiNW array surface is functionalized with the corresponding antibodies after the device is fabricated. The procedure for antibody functionalization of the SiNW surface is described in previous work.[21] A schematic illustration of the multiplexed detection of the OSCC biomarkers by the SiNW FET biosensor is shown in Fig. 2. The two SiNW sensors are separately functionalized with two different antibodies, after which the two biomarkers are applied to the SiNW surface. The binding events take place after specific recognition of the antibody-antigen, leading to a resistance change of the SiNW FET biosensor.

With acrylic wells fixed onto the chips, solutions containing probes or targets could be concentrated and localized around the SiNW sensor. In this way, the surface of the different SiNW arrays can be modified with the different antibody by locating the 4 individual wells onto the 4 SiNW clusters. In this work, amino-PEG was used to passivate any unreacted aldehydic groups so as to reduce non-specific protein bindings due to any multivalent hydrophobic interaction from PEG's repeating

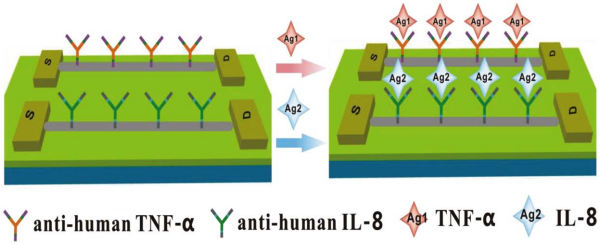

Fig. 2 Schematic diagram illustrating that the SiNW arrays are functionalized with two antibodies and two biomarkers are applied to the SiNW array surface by employing the acrylic wells on the different SiNW regions for solution exchange. The binding event takes place after specific recognition of the antibody-antigen, leading to a resistance change of the SiNW biosensor.

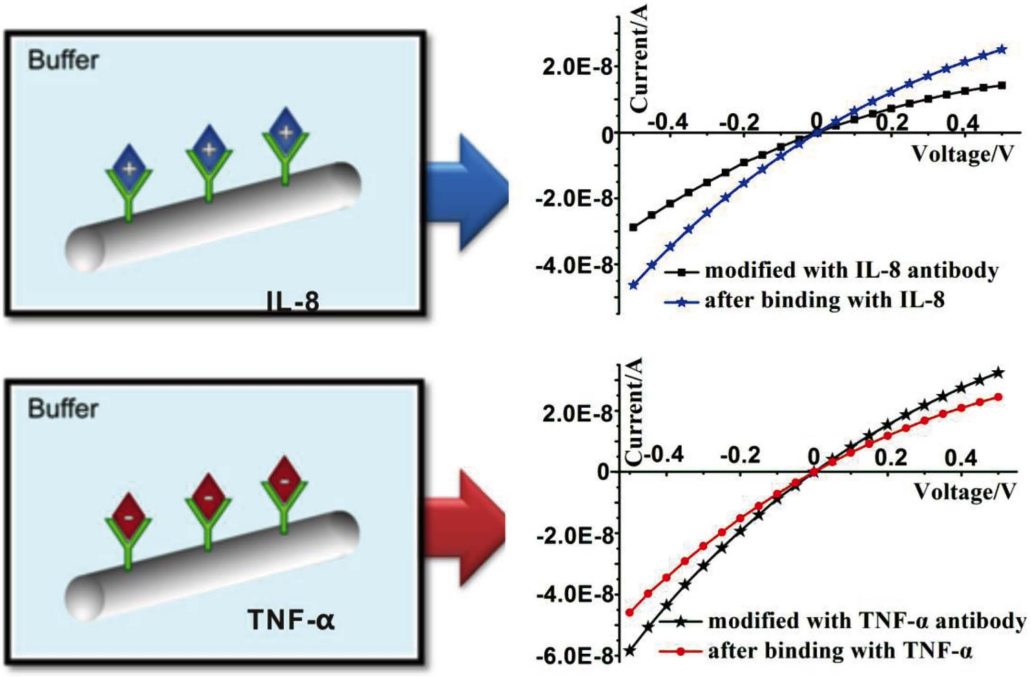

Fig. 3 Typical working I–V curves before and after IL-8 and TNF-α were bound to the corresponding antibodies immobilized on the different SiNW sensor surfaces. A positive charge inducing an accumulation of carrier in the SiNW bulk thus increases the conductance, while a negative charge present on the SiNW surface leads to a decrease of the conductance.

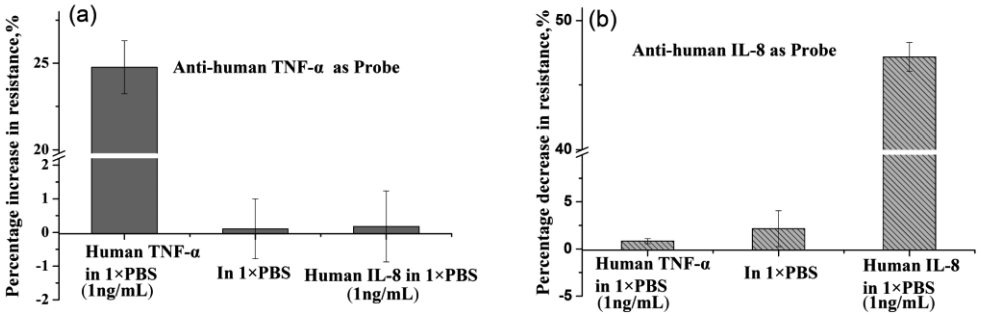

Fig. 4 (a) Averaged percentage increase in the resistance for 1 ng/mL human TNF-α, 1×PBS and 1 ng/mL human IL-8, respectively, with an anti-human TNF-α as probe. (b) Averaged percentage decrease in resistance for 1 ng/mL human IL-8, 1×PBS and 1 ng/mL human TNF-α, respectively, with anti-human IL-8 as the probe.

methylene units.[37]

After specific proteins are bound to these antibody-functionalized SiNW surfaces, the charges exhibited by these bound protein molecules in the measuring the buffer of a certain pH value can then directly affect the magnitude of current flow through the SiNW.[20] The isoelectric point (pI) of IL-8 is predicted to be 9.02, and the pI of TNF-α is within the range from 5.3 to 8.0.[38] Taking the Debye screening length into account, 0.01×PBS is selected as the measuring buffer due to its low ionic strength. Choosing a solution of 0.01×PBS of pH 8.5 as the measuring buffer, IL-8 has a net positive charge and TNF-α has a net negative charge. Because the SiNW used in this study is n-doped, the presence of a net positive charge on the nanowire results in the accumulation of carriers that subsequently leads to a decrease in the resistance. Conversely, the presence of a net negative charge causes a depletion of the SiNW bulk due to a repulsion between the similarly charged constituents, resulting in a resistance increase in this case. These changes can be detected by measuring the current before and after the event of probe-target binding. To investigate the current change by applying different biomarkers with various charges, IL-8 and TNF-α, respectively, were incubated with SiNW sensor surfaces that were functionalized with anti-IL-8 and anti-TNF-α, respectively. The I–V curves after functionalization with antibodies and interactions with target analytes are shown in Fig. 3. As can be seen in Fig. 3, the interaction between anti-human TNF-α and human TNF-α clearly resulted in an increased resistance. On the other hand, a decreased resistance was observed in the case of the interaction between anti-human IL-8 and human IL-8.

Selectivity

The complex components in saliva may interfere with the binding of the two biomarkers to the antibody-immobilized SiNW biosensor. To investigate the cross-reactivity of the present antibody-functionalized SiNW surface, three kinds of sample solutions containing 1 ng/mL IL-8, 1×PBS and 1 ng/mL TNF-α, respectively, were applied onto the two antibodies-functionalized SiNW surfaces. We then measured the response of the SiNW biosensor in the presence of the measuring solution. From the results shown in Fig. 4, it was observed that interaction between anti-human TNF-α and human TNF-α yielded a substantial increase in the resistance, averaging 24.77 ± 1.54%. The percentage changes of the two control groups, 1×PBS and human IL-8 in 1×PBS, are considerably negligible at 0.11 ± 0.89% and 0.179 ± 1.05%, respectively. As for the capturing of IL-8 by an anti-human IL-8 probe, an obvious decrease in the resistance (averaging 47.17 ± 1.13%) was obtained. The interaction of anti-human IL-8 with 1×PBS and human TNF-α, respectively, resulted in insignificant resistance changes of 2.16 ± 1.90% and 0.85 ± 0.26%. The low resistance change in all control groups indicates that the obvious resistance change arises from the specific binding of each protein to its corresponding antibody. These comparative results also show that the proposed SiNW FET biosensor has a satisfactory specificity.

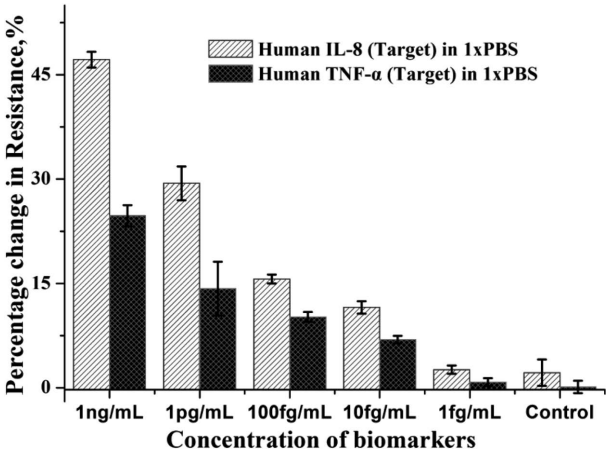

Fig. 5 Percentage change in the resistance *versus* different concentrations of IL-8 and TNF-α spiked in 1×PBS.

Comparing the magnitude of the percentage resistance change caused by the binding of IL-8 and TNF-α with their respective antibodies, the former pair gave a larger change. This could be due to the difference in the surface charge density exhibited by the two different proteins. Moreover, since the number of antibodies immobilized on each SiNW may differ by a small amount, the possible magnitude of the charge density can vary, thus inducing a slight disparity in the SiNW conductance.

Multiplexed detection of OSCC biomarkers in buffer

Next, we could achieve multiplexed detection of the OSCC biomarkers by incubating the sample solution containing the two biomarkers with the two antibodies-spotted SiNW sensors. To investigate the percentage change in the resistance of the SiNW to different concentrations, a 1×PBS solution spiked with the two biomarkers at different concentrations from 1 ng/mL to 1 fg/mL was applied onto the antibody-functionalized SiNW

Table 1 Comparison of different biosensors for IL-8 and TNF-α detection

Method	LOD	Solution	Target	Ref.
SPR	20.8 pg/mL	Saliva	IL-8	38
Multiplex immunoassay	100 pg/mL	Serum	IL-8	41
Electrochemical	8 pg/mL	Buffer	IL-8	42
Silicon photonic microring resonators	1 pg/mL	Cerebrospinal fluid	IL-8	43
Electrochemical	10 pg/mL	Buffer	TNF-α	44
SPR	11.6 pg/mL	Buffer	TNF-α	45
Resonance raman	90 fg/mL	Serum	TNF-α	46
Fiber optic particle plasmon resonance	8.22 pg/mL	Buffer	TNF-α	47
FET	10 fg/mL	Buffer	IL-8 and TNF-α	This work
FET	100 fg/mL	Saliva	IL-8 and TNF-α	This work

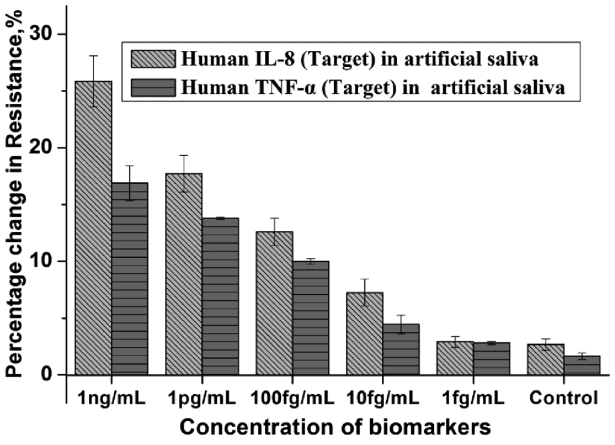

Fig. 6 Percentage change in the resistance *versus* different concentrations of IL-8 and TNF-α spiked in artificial saliva.

sensor separately. As shown in Fig. 5, the percentage change in the resistance was reduced upon decreasing the concentrations of the biomarkers used to interact with the antibody. This trend is within the expectation that a less amount of biomarkers in the target solution, the less the binding that takes place between the biomarkers and the antibodies immobilized on the SiNW. This would decrease the strength of the overall charge present on the surface of SiNW, and hence induce a change of the SiNW bulk to a smaller degree. The percentage change of the resistance caused by 1 fg/mL IL-8 and TNF-α, respectively, was around $0.801 \pm 0.58\%$ and $-2.592 \pm 0.598\%$, which is rather indistinguishable from that of the control groups. We thus defined the limit-of-detection (LOD) of the two biomarkers in 1×PBS measured by the SiNW FET biosensor as 10 fg/mL.

Multiplexed detection of OSCC biomarkers in saliva

In order to apply the SiNW FET biosensor for detecting the OSCC biomarkers in saliva, artificial saliva containing IL-8 and TNF-α at different concentrations were prepared and applied onto the antibody-functionalized SiNW FET biosensors. The limit of detection is determined when the signal of biomarkers is above three times the background signal. The percentage change in the resistance for 10 fg/mL IL-8 and TNF-α in artificial saliva was less than three-times the control response, as shown in Fig. 6. The LOD for the two biomarkers in artificial saliva was thus determined to be 100 fg/mL. As can be seen from Figs. 5 and 6, the standard deviations of ten independent measurements for each concentration were all less than 4%, revealing that the proposed biosensor has good repeatability. Comparing the results of the resistance change shown in Figs. 5 and 6, the percentage change in the resistance for the two biomarkers in artificial saliva was smaller than that in 1×PBS for different concentrations. The LOD in the buffer solution is thus one order of magnitude lower than the LOD in artificial saliva. This is mainly because artificial saliva has a more complex environment than the 1×PBS buffer.

The interference from artificial saliva certainly affects the sensitivity of the SiNW FET biosensor for both IL-8 and TNF-α. Even so, the SiNW devices still have a higher sensitivity than do other detection techniques, as shown in Table 1. As reported, the LOD of enzyme linked immunosorbent assay (ELISA) for IL-8 in buffer is 1 pM (8.3 pg/mL, the molar molecular weight of IL-8 is 8.3 kDa) and SPR achieves an LOD of 184 pM (1.5 ng/mL) for IL-8 in human saliva.[39] The LOD of ELISA for TNF-α was reported to be 0.48 pg/mL in the buffer.[40] Compared with other biosensors for the detection of IL-8 or TNF-α, our method has not only better sensitivity, but also multiplexed detection ability. The sensitivity of the SiNW FET biosensor for IL-8 and TNF-α could also satisfy the requirement of diagnosing the OSCC at a premature stage. More importantly, compared to the single biomarker test, which gives high probability of producing a false positive or negative result, the SiNW FET biosensor can achieve a multiplexed detection of biomarkers, which is necessary to provide higher accuracy of diagnosis.[48]

Conclusions

This paper has demonstrated the multiplexed sensing capabilities of the SiNW FET biosensor for the OSCC biomarkers, IL-8 and TNF-α, in a buffer solution and artificial saliva, respectively. The top-down lithography fabrication technique has been employed to yield well-aligned SiNW sensor arrays. The fabricated SiNW arrays include 51 clusters with 255 independently addressable sensors, theoretically allowing modification with a maximum of 51 types of antibodies. These clusters of SiNWs are functionalized with two different antibodies so that the multiplexed detection of the two biomarkers is carried out. With the LODs of both proteins being 10 fg/mL in the buffer solution and 100 fg/mL in artificial saliva, it has clearly shown that the SiNW FET biosensors are capable of detecting specific analytes even in ultra-low concentration. These results indicate that the established method used in this study not only has high specificity and sensitivity, but also is time-saving and cost-effective. With the advantages of label-free, sensitive, and multiplexed detection, the proposed method using the SiNW FET biosensor for detecting the two biomarkers in saliva is potentially a valid tool

for the early diagnosis of OSCC.

Acknowledgements

The authors thank Mr. Jun'An Jason Ang at Institute of Microelectronics, Singapore, for fabrication of the SiNW sensor chips. The authors also acknowledge financial support from the National Natural Science Foundation of China (Nos. 21275040 and 21475034), and the Natural Science Foundation of Hubei Province (No. 2013CFA061).

References

1. T. M. B. Rezende, M. d. S. Freire, and O. L. Franco, *Cancer*, **2010**, *116*, 4914.
2. Q. Wang, P. Gao, X. Wang, and Y. Duan, *Clin. Chim. Acta*, **2014**, *427*, 79.
3. M. A. R. St. John, Y. Li, X. F. Zhou, P. Denny, C. M. Ho, C. Montemagno, W. Y. Shi, F. X. Qi, B. Wu, U. Sinha, R. Jordan, L. Wolinsky, N. H. Park, H. H. Liu, E. Abemayor, and D. T. W. Wong, *Arch. Otolaryngol.*, **2004**, *130*, 929.
4. M. B. Lerner, J. D'Souza, T. Pazina, J. Dailey, B. R. Goldsmith, M. K. Robinson, and A. T. C. Johnson, *ACS Nano*, **2012**, *6*, 5143.
5. W. Ge, H.-L. Wang, and R.-P. Sun, *Eur. J. Pediatr.*, **2014**, *173*, 213.
6. D. Elashoff, H. Zhou, J. Reiss, J. H. Wang, H. Xiao, B. Henson, S. Hu, M. Arellano, U. Sinha, A. Le, D. Messadi, M. Wang, V. Nabili, M. Lingen, D. Morris, T. Randolph, Z. D. Feng, D. Akin, D. A. Kastratovic, D. Chia, E. Abemayor, and D. T. W. Wong, *Cancer Epidemiol., Biomarkers Prev.*, **2012**, *21*, 664.
7. N. L. Rhodus, V. Ho, C. S. Miller, S. Myers, and F. Ondrey, *Cancer Detect. Prev.*, **2005**, *29*, 42.
8. M. T. Arellano-Garcia, S. Hu, J. Wang, B. Henson, H. Zhou, D. Chia, and D. T. Wong, *Oral Dis.*, **2008**, *14*, 705.
9. K. Cheng, W. Zhao, S. Liu, and G. Sui, *Biomed. Microdevices*, **2013**, *15*, 949.
10. C. Y. Yang, E. Brooks, Y. Li, P. Denny, C. M. Ho, F. X. Qi, W. Y. Shi, L. Wolinsky, B. Wu, D. T. W. Wong, and C. D. Montemagno, *Lab Chip*, **2005**, *5*, 1017.
11. R. Sharma, R. E. Taylor, and L.-S. Bouchard, *J. Phys. Chem. C*, **2011**, *115*, 3297.
12. L. Tan, A. Wan, and H. Li, *ACS Appl. Mater. Intefaces*, **2013**, *6*, 18.
13. C.-S. Huang, S. George, M. Lu, V. Chaudhery, R. Tan, R. C. Zangar, and B. T. Cunningham, *Anal. Chem.*, **2011**, *83*, 1425.
14. S. Qu, J. Liu, J. Luo, Y. Huang, W. Shi, B. Wang, and X. Cai, *Anal. Chim. Acta*, **2013**, *766*, 94.
15. Y.-W. Huang, C.-S. Wu, C.-K. Chuang, S.-T. Pang, T.-M. Pan, Y.-S. Yang, and F.-H. Ko, *Anal. Chem.*, **2013**, *85*, 7912.
16. H. R. Jang, A. W. Wark, S. H. Baek, B. H. Chung, and H. J. Lee, *Anal. Chem.*, **2013**, *86*, 814.
17. S. Takahashi, K. Tsuji, T. Ueda, and Y. Okahata, *J. Am. Chem. Soc.*, **2012**, *134*, 6793.
18. G. Lamour, C. K. Yip, H. Li, and J. Gsponer, *ACS Nano*, **2014**, *8*, 3851.
19. F. Sun, T. Bai, L. Zhang, J.-R. Ella-Menye, S. Liu, A. K. Nowinski, S. Jiang, and Q. Yu, *Anal. Chem.*, **2014**, *86*, 2387.
20. J. H. Chua, R.-E. Chee, A. Agarwal, S. M. Wong, and G.-J. Zhang, *Anal. Chem.*, **2009**, *81*, 6266.
21. G.-J. Zhang, K. T. C. Chai, H. Z. H. Luo, J. M. Huang, I. G. K. Tay, A. E.-J. Lim, and M. Je, *Biosens. Bioelectron.*, **2012**, *35*, 218.
22. G.-J. Zhang, Z. H. H. Luo, M. J. Huang, J. A. J. Ang, T. G. Kang, and H. Ji, *Biosens. Bioelectron.*, **2011**, *28*, 459.
23. G.-J. Zhang, M. J. Huang, J. A. J. Ang, E. T. Liu, and K. V. Desai, *Biosens. Bioelectron.*, **2011**, *26*, 3233.
24. G.-J. Zhang, Z. H. H. Luo, M. J. Huang, G. K. I. Tay, and E.-J. A. Lim, *Biosens. Bioelectron.*, **2010**, *25*, 2447.
25. G.-J. Zhang and Y. Ning, *Anal. Chim. Acta*, **2012**, *749*, 1.
26. G.-J. Zhang, M. J. Huang, J. A. J. Ang, Q. Yao, and Y. Ning, *Anal. Chim. Acta*, **2013**, *85*, 4392.
27. B. Cai, S. Wang, L. Huang, Y. Ning, Z. Zhang, and G.-J. Zhang, *ACS Nano*, **2014**, *8*, 2632.
28. C. Tlili, N. V. Myung, V. Shetty, and A. Mulchandani, *Biosens. Bioelectron.*, **2011**, *26*, 4382.
29. C.-P. Chen, A. Ganguly, C.-Y. Lu, T.-Y. Chen, C.-C. Kuo, R.-S. Chen, W.-H. Tu, W. B. Fischer, K.-H. Chen, and L.-C. Chen, *Anal. Chem.*, **2011**, *83*, 1938.
30. G.-J. Zhang, M. J. Huang, Z. H. H. Luo, G. K. I. Tay, E.-J. A. Lim, E. T. Liu, and J. S. Thomsen, *Biosens. Bioelectron.*, **2010**, *26*, 365.
31. J.-Y. Kim, J.-H. Ahn, D.-I. Moon, T. J. Park, S. Y. Lee, and Y.-K. Choi, *Biosens. Bioelectron.*, **2014**, *55*, 162.
32. G. Zheng, F. Patolsky, Y. Cui, W. U. Wang, and C. M. Lieber, *Nat. Biotechnol.*, **2005**, *23*, 1294.
33. A. Fasoli and W. I. Milne, *Mater. Sci. Semicond. Process.*, **2012**, *15*, 601.
34. J.-H. Ahn, S.-J. Choi, J.-W. Han, T. J. Park, S. Y. Lee, and Y.-K. Choi, *Nano Lett.*, **2010**, *10*, 2934.
35. G.-J. Zhang, L. Zhang, M. J. Huang, Z. H. H. Luo, G. K. I. Tay, E.-J. A. Lim, T. G. Kang, and Y. Chen, *Sens. Actuators, B*, **2010**, *146*, 138.
36. S. C. Hamel, K. M. Ellickson, and P. J. Lioy, *Sci. Total Environ.*, **1999**, 243 - 244, 273.
37. B. Liu, P.-J. J. Huang, X. Zhang, F. Wang, R. Pautler, A. C. F. Ip, and J. Liu, *Anal. Chem.*, **2013**, *85*, 10045.
38. TNF (Human), Recombinant Human TNF, IL8 (Human), Recombinant Human Interleukin-8, **2010**, Creative BioMart.
39. C.-Y. Yang, E. Brooks, Y. Li, P. Denny, C.-M. Ho, F. Qi, W. Shi, L. Wolinsky, B. Wu, D. T. W. Wong, and C. D. Montemagno, *Lab Chip*, **2005**, *5*, 1017.
40. A. Bosnjakovic, M. K. Mishra, H. J. Han, R. Romero, and R. M. Kannan, *Anal. Chim. Acta*, **2012**, *720*, 118.
41. H. Ngo, H.-N. Wang, T. Burke, G. Ginsburg, and T. Vo-Dinh, *Anal. Bioanal. Chem.*, **2014**, *406*, 3335.
42. C. A. Ray, R. R. Bowsher, W. C. Smith, V. Devanarayan, M. B. Willey, J. T. Brandt, and R. A. Dean, *J. Pharm. Biomed. Anal.*, **2005**, *36*, 1037.
43. Y. Wan, W. Deng, Y. Su, X. Zhu, C. Peng, H. Hu, H. Peng, S. Song, and C. Fan, *Biosens. Bioelectron.*, **2011**, *30*, 93.
44. J. T. Kindt, M. S. Luchansky, A. J. Qavi, S.-H. Lee, and R. C. Bailey, *Anal. Chem.*, **2013**, *85*, 10653.
45. S. Weng, M. Chen, C. Zhao, A. Liu, L. Lin, Q. Liu, J. Lin, and X. Lin, *Sens. Actuators, B*, **2013**, *184*, 1.
46. J. Martinez-Perdiguero, A. Retolaza, L. Bujanda, and S. Merino, *Talanta*, **2014**, *119*, 492.
47. S. Laing, A. Hernandez-Santana, J. r. Sassmannshausen, D. L. Asquith, I. B. McInnes, K. Faulds, and D. Graham, *Anal. Chem.*, **2010**, *83*, 297.
48. Y.-C. Huang, C.-Y. Chiang, C.-H. Li, T.-C. Chang, C.-S. Chiang, L.-K. Chau, K.-W. Huang, C.-W. Wu, S.-C. Wang, and S.-R. Lyu, *Analyst*, **2013**, *138*, 4599.